![TU Delft logo]

Delft University of Technology

Microstructure evolution during high-temperature partitioning of a Medium-Mn Quenching and Partitioning steel

Ayenampudi, S.; Celada-Casero, C.; Sietsma, J.; Santofimia, M. J.

Important note
To cite this publication, please use the final published version (if applicable).
Please check the document version above.

Full Length Article

Microstructure evolution during high-temperature partitioning of a medium-Mn quenching and partitioning steel

S. Ayenampudi [a,*], C. Celada-Casero [a,b], J. Sietsma [a], M.J. Santofimia [a]

[a] Department of Materials Science and Engineering, Delft University of Technology, Mekelweg 2, 2628 CD Delft, The Netherlands
[b] Tata Steel Europe, IJmuiden Technology center, 1970 CA IJmuiden, The Netherlands

ARTICLE INFO

ABSTRACT

Medium-Mn Quenching & Partitioning (Q&P) steels have been recently considered as potential candidates for the 3rd generation advanced high-strength steels. The processing of these steels aims to induce the partitioning of substitutional alloying elements from martensite to austenite during an isothermal treatment at high temperature, where the diffusivity of substitutional alloying elements is sufficiently high. In this way, austenite increases its concentration of austenite-stabilising elements and thus its thermal stability. The present study aims to investigate the microstructural evolution during high temperature partitioning treatments in a medium-Mn steel and the possible occurrence of additional phase transformations that may compete with the process of atomic partitioning between martensite and austenite. Q&P routes in which the partitioning steps take place in the range of 400 °C–600 °C for times up to 3600 s were investigated. The final microstructures display an increased fraction of retained austenite with increasing holding times during partitioning at 400 °C, while at higher partitioning temperatures, 450 °C–600 °C, leads to cementite precipitation in austenite films and pearlite formation in blocky austenite, resulting in a decrease of the fraction of retained austenite with the holding time. This observation is supported with theoretical calculations of the volume change, suggesting that for maximising the fraction of retained austenite, short holding times are preferred during partitioning at high temperatures. Observations from the current study reveal that the successful application of high-temperature partitioning treatments in medium-Mn steels requires microstructure design strategies to minimize or suppress competitive reactions.

1. Introduction

The quenching and partitioning (Q&P) process, proposed by Speer and co-workers [1], has been considered as one of the most promising heat treatments for the production of third generation advanced high strength steels (AHSSs) with exceptional combination of strength and ductility. The typical Q&P process involves an initial austenitization (partial or full) followed by quenching to a temperature between the martensite start temperature (M_s) and room temperature to create a controlled fraction of primary martensite (M1). The steel is then reheated to a higher temperature to allow the carbon diffusion from the supersaturated martensite into the austenite, which is referred to as partitioning stage. The carbon enrichment of the austenite leads to its stabilization at room temperature. If part of the austenite is insufficiently enriched with carbon, this may transform into fresh martensite (M2) during the final quench to room temperature [2–4].

Speer et al. [4] proposed the constrained carbon equilibrium (CCE) model to describe the thermodynamics of the carbon partitioning pro-

cess. The CCE model is characterized by two assumptions: a) the carbon partitioning from martensite to austenite is finalized when the chemical potential of carbon in both phases is equal and b) the austenite/martensite interface is immobile during the partitioning step as the number of iron atoms in each phase are conserved. Typical partitioning temperatures in the Q&P process (350 °C–450 °C) are relatively low and the diffusivities of substitutional alloying elements during the partitioning step can be ignored at the time ranges that are normally considered. Therefore, most studies are concentrated on studying the stabilization of austenite by carbon [2,5–8].

Recently, the idea of stabilizing the austenite through Q&P heat treatments in which the partitioning stage takes place at temperatures high enough to stimulate the partitioning of substitutional alloying elements has been proposed by some authors [9–13]. This possibility stems from the observation of an apparent partitioning of substitutional alloying elements at relatively low temperatures. For example, Santofimia et al. [9] reported the partitioning of manganese at typical partitioning conditions (400 °C for 50 s) at some martensite/austenite interfaces.

Later, several authors [10–13] observed that the range of manganese partitioning is increased with the increase in partitioning temperature from 400 °C to 450 °C. Some of the recent works [14,15] also aimed at investigating austenite stability in the intercritical range of temperatures by promoting austenite reverse transformation. However, manganese tends to partition into austenite only a few nanometres (typically less than 10 nm) after isothermal holding times of up to 1 h at these temperatures. Therefore, the partitioning ranges of manganese reported earlier may not be sufficient to stabilize the entire films of retained austenite, which typically have a thickness 5–20 nm.

The diffusivity of manganese in austenite, at typical Q&P temperatures (400 °C–450 °C), is in the order of magnitude of 10^{-26} m²/s [16], which is very low compared to that of carbon, which is around 10^{-16} m²/s [17]. In order to promote manganese partitioning from martensite into austenite it is important to apply higher partitioning temperatures. However, higher isothermal holding temperatures may increase the probability of occurrence of competitive reactions like austenite decomposition into bainite or pearlite, or carbide formation [18] or austenite reverse transformation [14–15]. Most of the earlier works reported the occurrence of bainite formation [3] and carbide precipitation inside primary martensite [6,8] during isothermal holding at lower partitioning temperatures (400 °C–450 °C). However, there are no research works focused on the microstructural development that takes place during partitioning steps at higher temperatures (500 °C–600 °C) below the intercritical region. Hence, the current research aims to gain insight into the microstructural evolution and competitive reactions occurring in a medium-Mn steel during partitioning at temperatures of 400 °C–600 °C and times ranging from 180 s to 3600 s. The results of this study open up the possibility to new Q&P microstructural design strategies in medium-Mn steels that minimize or suppress the occurrence of competitive reactions during high-temperature partitioning treatments.

2. Materials and experimental methods

The chemical composition of the medium-Mn steel used in this study is shown in Table 1. The content of manganese is expected to contribute to the stabilization of the austenite and to delay significantly the formation of structures such as ferrite, bainite and Widmanstätten ferrite during cooling to the quenching temperature. Silicon is normally used to delay any cementite precipitation during the partitioning step.

The steel was produced in the form of a forged billet. Cylindrical specimens of 10 mm in length and 4 mm in diameter were machined from the forged billet. These specimens were heat treated in a Bähr 805 DIL A/D dilatometer. A type S thermocouple spot-welded on the surface was used to monitor and control temperature. Low pressure on the order of 10^{-4} mbar was used during heating or isothermal segments, and helium was used as the coolant. The error in change in length from dilatometry experiments was estimated as ± 0.01 %.

The applied thermal routes are shown in Fig. 1. These thermal routes include a full austenitization at 950 °C during 120 s, quenching at 30 °C/s to 190 °C and partitioning at temperatures (T_P) ranging from 400 °C to 600 °C for partitioning times (t_P) of up to 3600 s. In the following sections, conditions will be indicated as QP T_P - t_P for concise identification of specimens. A heat treatment involving a direct quench from austenitization conditions was also included in the investigations.

After the application of the heat treatments, the specimens were cut into half and the surface was prepared by grinding with P800, P1000, and P1200 abrasive papers and polishing with 6, 3 and 1 μm diamond paste. The polished specimens were etched with a 2 % Nital solution for
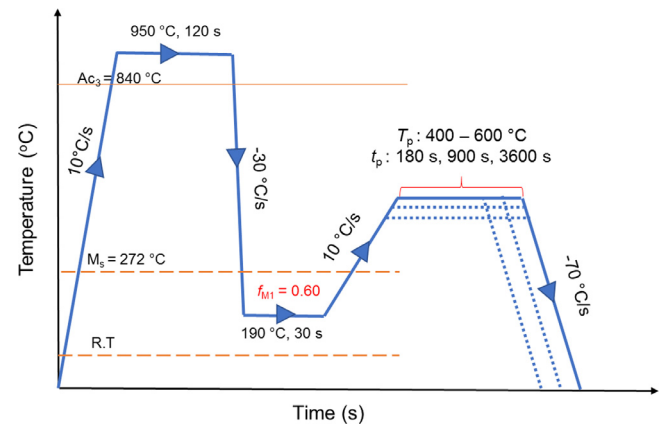
Table 1
Chemical composition (wt. %) of the steel investigated.

C	Mn	Si	Mo	Al	Cr	Fe
0.31	4.58	1.52	<0.005	0.01	0.02	Balance

Fig. 1. Schematic drawing of the Quenching and Partitioning heat treatments.

the subsequent observation using scanning electron microscopy (SEM), for which a JEOL JSM-6500F field emission gun scanning electron microscope (FEG-SEM), operating at 15 kV, was used.

The volume fractions (f_{RA}) and lattice parameter (a_γ) of retained austenite were determined by means of X-ray diffraction (XRD) analysis using a Bruker type D8-Advance diffractometer, in a 2θ range from 40° to 130°, with Co Kα radiation (wavelength 0.1789 nm), using a step size of 0.042⁰ 2θ, with a counting per step of 3 s. This 2θ range covers the (110), (200), (211), (220) ferrite peaks and the (111), (200), (220), (311) austenite peaks. The volume fraction of retained austenite and the errors in determining the retained austenite fraction were calculated by the direct comparison method of austenite and martensite peaks using the procedure described by Jatczak [19]. In the present work, volume fractions of retained austenite below 0.03 are neglected as this is the detection limit of the X-ray diffraction measurements. The carbon concentration within the retained austenite is calculated from its lattice parameter, a_γ (in Å) using the method described in [20]:

$$a_\gamma = 3.556 + 0.0453 \cdot x_C + 0.00095 \cdot x_{Mn} + 0.00157 \cdot x_{Si} \qquad (1)$$

where x_i, represents the concentration of the alloying element i in wt. %.

Magnetization measurements were performed at room temperature on cubic specimens of 2.0 mm in side length that were machined from the centre of heat-treated dilatometry specimens. A 7307 vibrating sample magnetometer, calibrated with a National Institute of Standards and Technology nickel specimen, was used. With this equipment, magnetization curves at room temperature were measured by a stepwise change in the applied magnetic field from +1.6 to −1.6 T. The saturation magnetization values were obtained by fitting the approach to the saturation of the experimentally obtained magnetization curve, according to Ref. [21]. The volume fraction of martensite (f_M) in the quenched specimen is determined by comparing the saturation magnetization values obtained both on the specimen with martensite to be measured and on pure Fe-BCC specimens according to the method indicated in Ref. [21].

3. Results

In this section, the microstructural evolution during the different applied Q&P heat treatments is evaluated based on the dilatometry measurements, X-ray diffraction analysis, magnetisation measurements and microstructural observations.

The volume fraction of martensite formed at the quenching temperature was determined by analysing the dilatometry response of the as-quenched specimen austenitized at 950 °C for 120 s and directly quenched to room temperature, as Fig. 2a shows. The linear expansion behaviour of the BCC and FCC lattices in the dilatometry curve were used to fit the thermal expansion of both phases. In order to extract
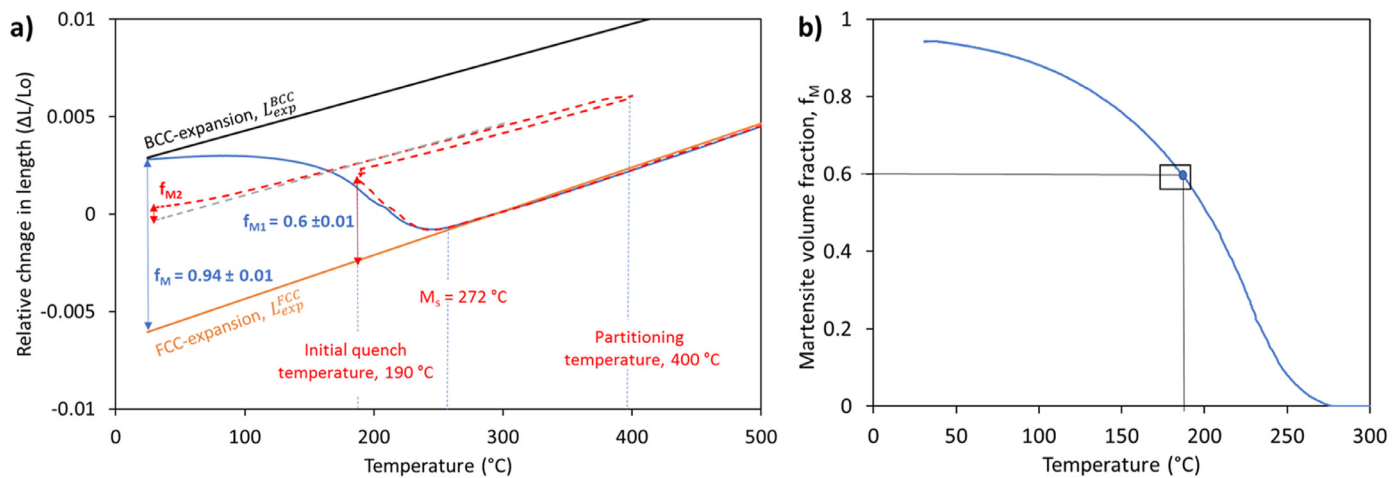
Fig. 2. (a) Relative change in length versus temperature of an as-quenched (solid blue line) and QP400-3600 (dashed red line) specimens. f_M is the volume fraction of martensite formed after an as-quench heat treatment; f_{M1} and f_{M2} are the volume fractions of primary and fresh martensite formed during QP400-3600 heat treatment, respectively (b) Volume fraction of martensite as a function of temperature obtained applying the lever rule to the as-quench dilatation curve.

information regarding the phase fractions formed during the quench, the final change in length is associated with the formation of a volume fraction of martensite equal to 0.94 ± 0.01, as experimentally measured using the magnetometer. By applying the lever rule, the volume fraction of martensite is determined as a function of the temperature during the quenching treatment, as indicated by a solid blue line in Fig. 2b. According to this data, the selected quenching temperature of 190 °C corresponds with the formation of a volume fraction of primary martensite (M1) equal to 0.60 ± 0.01, leaving a volume fraction of untransformed austenite of 0.40 ± 0.01. These volume fractions of primary martensite and, consequently, austenite were chosen with the aim to stabilize a significant volume fraction of austenite in the final microstructures, as the steel has relatively high carbon content.

Fig. 2a also shows the dilatation curve of QP400-3600 (dashed line) specimens, as an example. This dilatometry curve of QP400-3600 specimen is used to explain the microstructural development during the Q&P processing routes. Initially, a linear contraction is detected corresponding to the cooling from the austenitization temperature. When the temperature decreases below the M_s and until the quench temperature (T_Q), a dilatation corresponding to the formation of 0.60 volume fraction of athermal martensite is observed. Then, the specimen is reheated to 400 °C, during which an expansion is observed, indicating no phase transformations. The small positive change in length observed during the isothermal holding at 400 °C is caused by the formation of carbides and/or pearlite and to the carbon partitioning from martensite to austenite, and it will be discussed in detail in the following sections. During the partitioning step, part of the remaining austenite enriches sufficiently in carbon to be thermally stabilized at room temperature. A small deviation from linearity of the dilatometric curves during the final quench to room temperature indicates the formation of a small volume fraction of fresh martensite (M2) from the less stable austenite. The volume fractions of fresh martensite (f_{M2}) were determined by comparing the measured change in length with the change in length observed in the direct-quenched specimen as explained in the ref. [22,23]. The retained austenite volume fractions (f_{RA}) in the final Q&P microstructures were measured using X-ray diffractometry as explained in the experimental procedure. The remaining constituents in the final microstructures will be carbides and/or pearlite. The total volume fraction of these constituents, f_{c+p}, was calculated by balance of the phase fractions:

$$f_{M1} - f_{M2} - f_{RA} - f_{c+p} = 1 \qquad (2)$$

The same method was applied to determine the volume fraction of phases present all final Q&P microstructures. The results are displayed

on the left-hand side of Fig. 3. Also, on the left-hand side of Fig. 3, the dilatometry curves against time registered during the partitioning steps for 3600 s are represented. In the following, this information will be employed together with the microstructural observations in order to understand the microstructural evolution taking place during the partitioning step at the different studied temperatures.

3.1. Partitioning at 400 °C

Fig. 3a shows the change in length observed in the dilatometry specimens during the isothermal holding at 400 °C for 3600 s. The dilatometry curve shows two stages. The first stage is an expansion, which is observed during approximately the first 1800s. This expansion is related to the process of carbon partitioning from the carbon-supersaturated martensite (M1) into the austenite [24]. The second stage is a slight contraction, which is likely due to the precipitation of carbides in primary martensite, as previously observed by Toji et al. [13].

The final microstructures show an increase in the volume fraction of retained austenite and a decrease in the volume fraction of fresh martensite with increasing holding times. This evolution results from the process of carbon partitioning from martensite to austenite, which progressively stabilizes the austenite during the partitioning step.

Fig. 3b shows the microstructure of the specimen after partitioning at 400 °C for 3600 s. The primary martensite is characterised by the presence of carbides. The microstructure also show blocky islands of fresh martensite/retained austenite (MA islands) with a thickness of few micrometres. Nanometric retained austenite films are also observed in between the martensite laths.

3.2. Partitioning at 450 °C

The dilatometry curve during the partitioning step at 450 °C for 3600 s is shown in Fig. 3c. A small expansion is observed within the first 40 s (zoomed- in the inset), which is related to carbon partitioning. After 40 s, a continuous decrease in length is observed, which may be related with a more pronounced precipitation process than that observed during partitioning at 400 °C. Kannan et al. [25] and Onink et al. [26] observed that austenite films saturated with carbon tend to decompose into carbon-depleted austenite and cementite, and this phenomenon is accompanied by contraction.

After partitioning at 450 °C, the final volume fractions of microstructural constituents indicate a simultaneous increase in the volume fraction of fresh martensite and a decrease in the volume fraction of retained
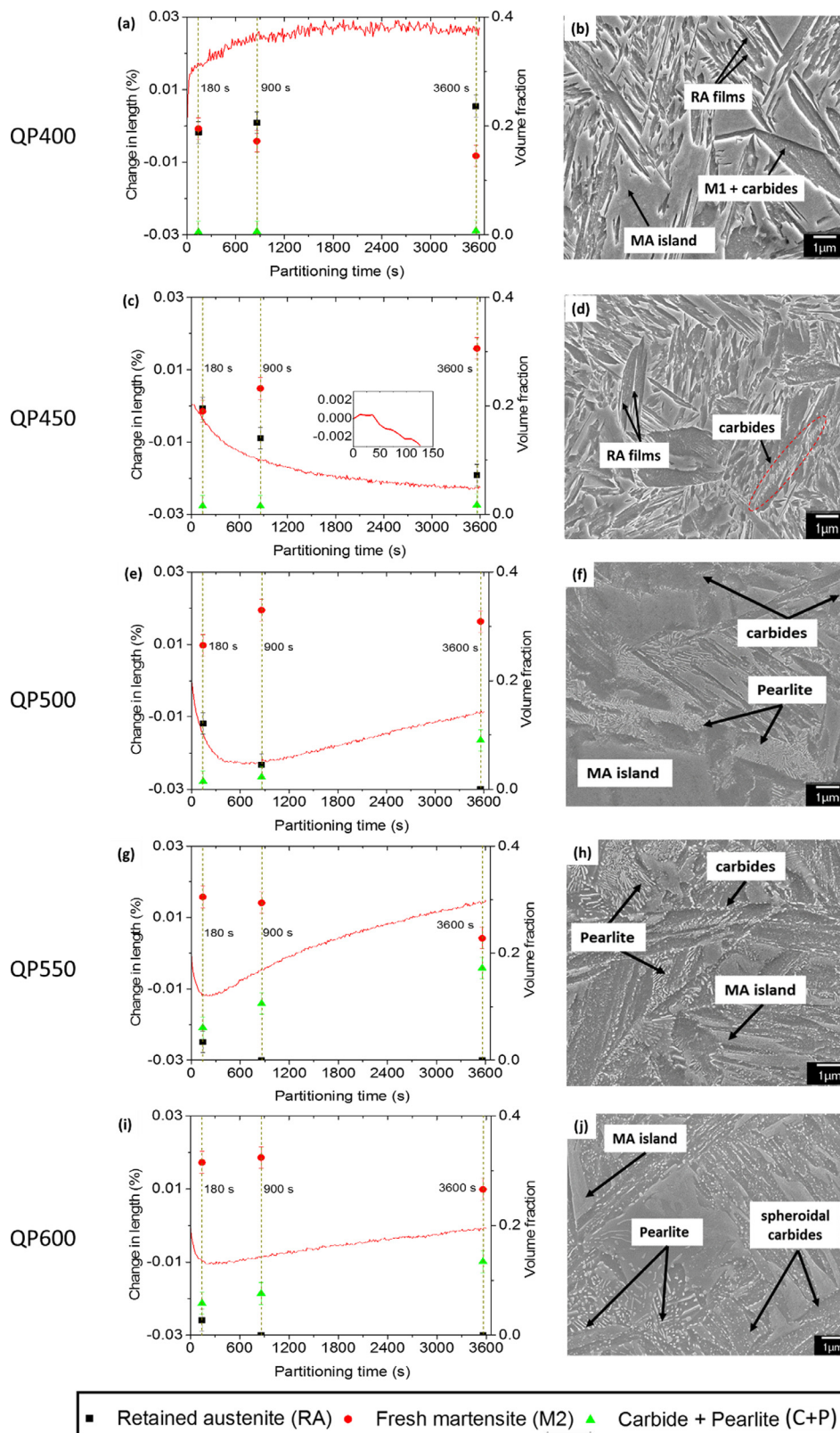
Fig. 3. For every partitioning temperature, the figures on the left show the change in length and the volume fraction of phases present at the end of the different Q&P heat treatments as a function of the partitioning time. Figures on the right side show microstructures of the specimens observed under the SEM after partitioning for 3600 s at partitioning temperatures of 400 °C–600 °C.

austenite. After partitioning for 3600 s at 450 °C, the volume fraction of retained austenite is essentially the same as that present in the as-quenched state.

Fig. 3d shows a SEM micrograph of the specimen partitioned at 450 °C for 3600 s. In this case, the precipitation of carbides inside

primary martensite is not very evident. Arrays of parallel carbides aligned in the direction of the martensite laths can be clearly observed in the primary martensite, as indicated in Fig. 3d with dashed lines. These arrays of carbides appear to occupy the locations where austenite films were observed at shorter partitioning times.

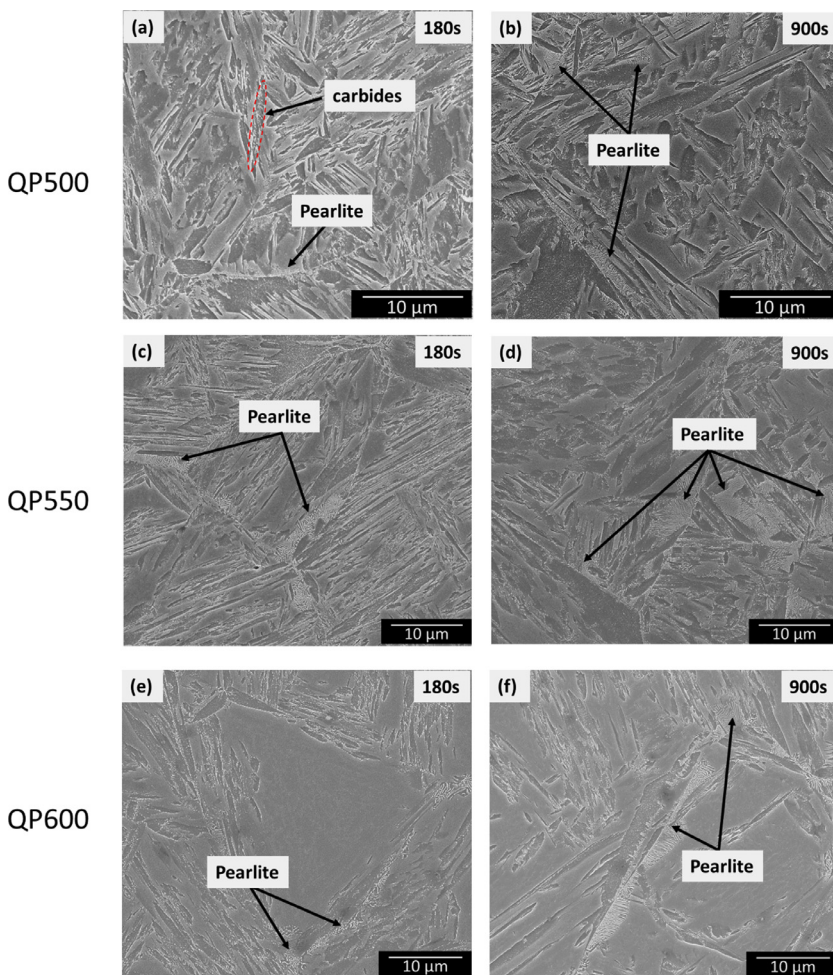**Fig. 4.** The figures on the left and right show microstructures of the specimens observed under the SEM after partitioning at temperatures of 500 °C, 550 °C and 600 °C for 180 s and 900 s, respectively. Evolution of microstructural features with partitioning time and temperature are shown in this figure.

3.3. Partitioning at 500 °C

The dilatometry curve corresponding to partitioning at 500 °C shows a decrease in change in length for the first 600 s (Fig. 3e). This contraction is of the same order of magnitude as the one observed during partitioning at 450 °C (Fig. 3c) although in the present case it occurs in a shorter time. This contraction is followed by a continuous dilatation until the end of the partitioning stage.

Fig. 3e shows that, with the increase in holding time, the volume fraction of retained austenite decreases continuously until it is not detected by X-ray diffraction after partitioning for 3600 s. This decrease in the retained austenite volume fraction coincides with the increase in the volume fraction of fresh martensite, carbides and pearlite.

The microstructure of the specimen after partitioning at 500 °C for 3600 s (Fig. 3f) shows the presence of pearlite in the microstructure. This suggests that the increase of change in length observed in the dilatometry curve is related to pearlite formation, which becomes the dominant process after 900 s of isothermal holding, as can be seen from the SEM micrographs, Fig. 4a and 4b. Precipitation of carbides is observed at the phase boundaries of fresh martensite/retained austenite islands with the surrounding primary martensite.

3.4. Partitioning at 550 °C

The dilatometry curve during partitioning at 550 °C (Fig. 3g) shows a very similar behaviour as the one at 500 °C. However, in the present case, the transition from contraction to expansion occurs at a shorter holding time (200 s) and the magnitude of the contraction is smaller.

Moreover, the final expansion observed in the dilatometry curve is higher than in the case of partitioning at 500 °C.

The evolution of phase fractions in the final microstructure presented in Fig. 3g shows that no retained austenite is detected by XRD after 900 s of partitioning, while the volume fraction of carbides and pearlite significantly increases with increasing the holding time which is also evident from the SEM micrographs, Fig. 4c and 4d.

The SEM micrograph of the specimen partitioned at 550 °C for 3600 s (Fig. 3h) shows a dense distribution of pearlite in the final microstructure, whereas the fresh martensite/retained austenite islands (MA islands) are less evident in the present case than after partitioning at 500 °C.

3.5. Partitioning at 600 °C

The dilatometry curve registered during partitioning at 600 °C for 3600 s, Fig. 3i, is very similar to the one observed during partitioning at 550 °C. However, the specimen partitioned at 600 °C experiences a smaller expansion than in the case of partitioning at 550 °C, indicating the formation of a lower volume fraction of pearlite.

The final volume fractions also show similar trends with the partitioning time as the ones observed during partitioning at 550 °C. That is, a low volume fraction of retained austenite that becomes undetectable by XRD after partitioning for 900 s and a simultaneous increase of the volume fraction of carbides and pearlite with partitioning time.

Pearlite is also observed in the SEM micrograph of the specimen partitioned at 600 °C for 3600 s (Fig. 3j). SEM micrographs, Fig. 4b - 4f, indicate that pearlite formation during partitioning stage is more

significant at 550 °C than at 600 °C. Moreover, carbides in primary martensite observed at 600 °C seem to be coarser than after partitioning at 550 °C, Fig. 3j. Besides pearlite, lamellar carbides are observed in the fresh martensite/retained austenite islands after partitioning at 600 °C.

4. Discussion

The previous section has presented a qualitative description of the microstructural evolution taking place during the partitioning step at the different studied temperatures. In this section, a quantitative assessment is performed in order to evaluate the extent to which microstructural processes hinder or inhibit the partitioning of carbon and substitutional alloying elements from the martensite into the austenite and, therefore, promote an adequate stabilization of the austenite at room temperature. For this purpose, firstly, the redistribution of carbon among phases and due to phase transformations during the partitioning stage is analysed based on the carbon balance at different partitioning temperatures. Then, the sequence of microstructural mechanisms occurring at different partitioning temperatures is validated through theoretical calculations of the length change. Finally, it is discussed how simultaneous microstructural phenomena during partitioning influence the stabilisation of the austenite at different temperatures and the most promising routes are identify.

4.1. Carbon balance at different partitioning temperatures

It is crucial to understand how carbon redistributes in the microstructure during the partitioning stage to understand the stabilisation process of the austenite. Therefore, in this section, the carbon distribution is quantified by the analysis of the carbon content of all microstructural constituents present in the microstructures after Q&P heat treatments in which the partitioning time lasted for 3600 s. This evaluation provides information on the effectiveness of the carbon partitioning from martensite to austenite in order to stabilize austenite at room temperature.

The carbon content in the phases at the very beginning of partitioning stage ($t_p = 0$ s) can be represented by:

$$\bar{x} = f_{\gamma(t_p=0)} \cdot x_{\gamma(t_p=0)} + f_{M1(t_p=0)} \cdot x_{M1(t_p=0)} \quad (3)$$

where $\bar{x}$ is the total carbon content present in the alloy (0.31 wt. %), f_γ and f_{M1} are the volume fractions of austenite and martensite present at the beginning of the partitioning stage (0.40 and 0.60 respectively), and x_γ and x_{M1} are the carbon concentrations present in austenite and martensite at the beginning of the partitioning stage. Since the martensitic transformation is diffusionless and considering that there is no change in carbon concentration during the reheating stage, martensite and austenite are assumed to have the same carbon content (0.31 wt. %) at the onset of the partitioning stage. These initial conditions at the beginning of the partitioning stage are considered equal for all studied Q&P heat treatments.

Section 3 has shown that, during the partitioning step, several competitive phenomena occur at different stages of the isothermal holding depending on the partitioning temperature. These phenomena are carbide precipitation in martensite, pearlite formation, carbide precipitation in austenite and carbon enrichment of the austenite. All these phenomena compete for the carbon available in the microstructure. Therefore, after 3600 s of partitioning, the following carbon balance can be applied:

$$\bar{x} = f_{\gamma(t_p=1h)} \cdot x^\gamma_{c(t_p=1h)} + f_{M1(t_p=1h)} \cdot x^{M1}_{c(t_p=1h)} + f_{p(t_p=1h)} \cdot x^p_{c(t_p=1h)} + X_c \quad (4)$$

where $\bar{x}$ is the total fraction of carbon present in the alloy (0.31 wt. %), f_i and x^i_c represent the volume fraction and carbon content of phase i ($i = \gamma$, M1 and P) after 3600 s of isothermal holding and before the final quench to room temperature and X_c is the total fraction of carbon that is precipitated in carbides.

The volume fraction of austenite at the end of the partitioning step and before the final quench, f_γ, can be calculated as the sum of volume fractions of retained austenite and fresh martensite observed in the final microstructures. The corresponding carbon content (x^γ_c) is calculated considering the carbon content in retained austenite (x^{RA}_c) measured by X-ray diffractometer and the carbon content in fresh martensite (x^{M2}_c). This balance can be formulated as:

$$f_{\gamma(t_p=1h)} \cdot x^\gamma_{c(t_p=1h)} = f_{RA} \cdot x^{RA}_C + f_{M2} \cdot x^{M2}_C \quad (5)$$

where f_{RA} and f_{M2} are the volume fractions of retained austenite and fresh martensite, respectively.

The carbon content in fresh martensite (x^{M2}_c) is determined based on the martensite start temperature during the final quench (experimental curve) and applying the Rowland and Lyle equation [27] that relates the martensite start temperature (in °C) with the chemical composition of the alloy. In the present study the equation has been adapted to the chemical composition of the steel as

$$M_s = 499 - 324 \cdot x^{M2}_c - 32.4 \cdot x_{Mn} - 27 \cdot x_{Cr} - 10.8 \cdot x_{Si} - 10.8 \cdot x_{Mo} \quad (6)$$

where x_i represents the concentration of element i ($i = C$, Mn, Cr, Si and Mo) in the alloy in wt. %.

The carbon content in solid solution in primary martensite, x^{M1}_c, is assumed to be zero after 3600 s of partitioning time at all studied partitioning temperatures due to the formation of carbides in the matrix and the carbon partitioning to austenite. The carbon content in pearlite is assumed to be the eutectoid carbon content.

Under these assumptions, the combination of Eqs. (4)–(6) provides information regarding the carbon present in every microstructural constituent and in carbides after 3600 s of partitioning at all studied temperatures. The results and details of the numerical values used in the calculations are presented in Table 2 and are explained by partitioning temperature hereafter.

4.1.1. Partitioning at 400 °C

During the isothermal holding at 400 °C for 3600 s, carbon partitioning from martensite to austenite and carbide precipitation in primary martensite occur in the microstructure. Pearlite formation is not observed. With this information, the application of Eq. (4) reveals that the fraction of carbon that precipitates in the form of carbides (X_C) in primary martensite is around 0.01 wt% C.

4.1.2. Partitioning at 450 °C

During partitioning at 450 °C, carbide precipitation in austenite films takes place along with carbon partitioning from martensite to austenite and carbide precipitation in primary martensite. In this case, the balance of carbon shows that the fraction of carbon that precipitates in carbides, X_C, is around 0.08 wt% C, which is higher than that observed in the case of partitioning at 400 °C and coincides with the microstructural observations.

4.1.3. Partitioning at 500 °C, 550 °C and 600 °C

Partitioning at 500 °C, 550 °C and 600 °C promotes pearlite formation along with carbon partitioning from martensite to austenite, carbide precipitation in primary martensite and carbide precipitation in austenite. The carbon balance shows that the fraction of carbon that precipitates in the form of carbides, X_C, is around 0.11 wt. % in the case of partitioning at 500 °C and 550 °C, and of 0.12 wt% in the case of partitioning at 600 °C.

The maximum volume fraction of pearlite is observed after partitioning at 550 °C (Fig. 3). This coincides with the nose of the pearlite formation in the theoretically calculated Temperature-Time-Transformation diagram, using the free program MUCG83 [28].

Table 2
Volume fraction and carbon content of phases present at the end of the partitioning step for different partitioning temperatures. These phases are carbon enriched austenite (γ), primary martensite (M1), pearlite (p) and carbides (X_c). The Table also shows the volume fractions and carbon contents of fresh martensite (M2) and retained austenite (RA) used for the estimation of the volume fraction (f_γ) and carbon content x_c^γ of carbon enriched austenite (γ) present after 3600 s of partitioning time.

(T_P°C)	C enriched austenite					C depleted martensite		Pearlite		Carbides
	f_γ	x_c^γ (wt. %)				f_{M1}	x_c^{M1} (wt. %)	f_p	x_c^p (wt. %)	X_c (wt. % C)
		M2		RA						
		x_c^{M2}	f_{M2}	f_{RA}	x_c^{RA}					
400	0.39	0.68	0.16	0.23	0.80	0.6	0	0	0	0.01
450	0.39	0.58	0.32	0.07	0.60			0	0	0.08
500	0.31	0.45	0.31	–	–			0.08	0.73	0.11
550	0.22	0.32	0.22	–	–			0.17	0.73	0.11
600	0.27	0.35	0.27	–	–			0.12	0.73	0.12

4.2. Length changes associated to the reactions during the partitioning stage

The focus of this section is on the evaluation and validation of the influence of each microstructural mechanism on the overall change in length observed at the end of the partitioning process. This provides insight into the sequence of the microstructural processes occurring at different partitioning temperatures. According to the mechanisms proposed in the previous section based on the dilatometry results and microstructural observations and using the phase volume fractions and carbon contents calculated in Table 2, the theoretical change in length associated to each microstructural process during the partitioning stage are calculated and compared with the experimental values.

The relation between the relative change in length recorded during a dilatometry experiment and the actual change in volume that develops in the material can be expressed as:

$$\frac{\Delta L}{L_i} = \frac{1}{3} \cdot \frac{V^f - V^i}{V^i} \tag{7}$$

where $\Delta L = L_f - L_i$ is the difference between the final (L_f) and initial (L_i) length of the material after and before (the partitioning stage. V^f and V^i are the total specific volumes of the material after and before the partitioning stage, respectively. In the present analysis, the initial state, i, represents the starting point of the partitioning step ($t_p = 0$ s) and the final stage, f, represents the end of the partitioning stage after 3600 s ($t_p = 3600$ s).

The total specific volume, V, of the material at any stage of the isothermal holding can be expressed as:

$$V = \sum_j v_j \cdot f_j \tag{8}$$

where v_j and f_j are the specific volume and volume fraction of every microstructural constituent, j. In this context, the phases present in the microstructure at the beginning of partitioning stage ($t_p = 0$ s) are primary martensite and untransformed austenite, whereas the microstructural constituents that are present at the end of the partitioning step ($t_p = 3600$ s) depend on the partitioning temperature (see Table 2).

Eq. (7) can be rewritten including the specific volumes, as expressed in Eq. (8), of all possible individual phases at the beginning and at the end of the partitioning step as:

volume fraction of pearlite and carbides are estimated from carbon balancing (Eq. (4)) as explained in Section 4.1.

The specific volumes of the crystal structures are calculated from the corresponding lattice parameters and thermal expansion coefficients according to the formulae presented in Table 3. The lattice parameters of a particular crystal structure at a given partitioning temperature, T, can be calculated using the following equation:

$$a_{lattice,\,T} = a_{lattice,\,RT} \cdot (1 + \beta \cdot (T - 300\ K)) \tag{10}$$

where β is the thermal expansion coefficient, $a_{lattice,\,T}$ and $a_{lattice,\,RT}$ are the lattice parameters at the partitioning temperature and room temperature (300 K), respectively. Lattice parameters at room temperature $a_{lattice,\,RT}$ for austenite (γ), martensite ($\alpha^|$) and cementite (θ) are calculated as a function of chemical composition (in at.%) and are shown in Table 3.

Depending on the phenomena observed at each partitioning temperature, Eq. (9) is modified accordingly to calculate theoretical changes in length.

For the theoretical calculations of change in length, carbide precipitation in primary martensite is neglected at all partitioning temperatures, as the volume fraction of carbides formed at 400 °C is lower than 0.01 and even lower at higher partitioning temperatures (450 °C – 600 °C).

During partitioning at high temperatures (450 °C–600 °C), precipitation of carbides inside austenite is observed. Through EBSD phase maps, Kannan et al. [25], observed that the nature of carbide precipitated inside austenite during isothermal holding at 500 °C is cementite (6.67 wt. %). By means of ThermoCalc calculations and Dictra simulations of the carbon redistribution between martensite and austenite during partitioning at 500 °C, it has been recently shown that the carbon content of austenite-films in between martensite laths can reach values above 1.50 wt. % C in less than 1 s [35]. This carbon content in austenite is well above that at which the molar Gibb's free energy of austenite and ferrite are equal at 500 °C (0.48 wt. % C). This means that, within the range of temperatures of 450 °C–600 °C, the austenite might be sufficiently supersaturated in carbon so that cementite can form, causing carbon impoverishment in the surrounded austenite. Fig. 3 showed that, at 450 °C, this process causes a continuous contraction over 1 h of

$$\frac{\Delta L}{L_o} = \frac{1}{3} \cdot \frac{\{(\vartheta_\gamma^f \cdot f_\gamma^f + \vartheta_{M1}^f \cdot f_{M1}^f + \vartheta_p^f \cdot f_p^f + \vartheta_{carbides}^f \cdot f_{carbides}^f) - (\vartheta_\gamma^i \cdot f_\gamma^i + \vartheta_{M1}^i \cdot f_{M1}^i)\}}{(\vartheta_\gamma^i \cdot f_\gamma^i + \vartheta_{M1}^i \cdot f_{M1}^i)} \tag{9}$$

where ϑ_γ^i, ϑ_{M1}^i and f_γ^i, f_{M1}^i are the specific volumes and volume fractions of austenite and martensite before partitioning stage. ϑ_γ^f, ϑ_{M1}^f, ϑ_p^f, $\vartheta_{carbides}^f$ and f_γ^f, f_M^f, f_p^f, $f_{carbides}^f$ stands for the specific volume and volume fraction of carbon enriched austenite, primary martensite, pearlite and carbides at the end of partitioning stage, respectively. In the above equation, volume fraction of austenite and primary martensite are quantified from experimental techniques. While,

partitioning time, whereas, at 500 °C, a similar contraction in magnitude occurs predominantly during the first 600 s. Therefore, under this assumption, calculations show that the volume fraction of cementite precipitated in austenite at all partitioning temperatures is around 0.01. For the theoretical change in length calculations at partitioning temperatures of 500 °C – 600 °C, pearlite ($\gamma \rightarrow \alpha + \theta$) is also included as it was also observed during the partitioning stage.

Table 3
Equations used to calculate the specific volume and lattice parameter of martensite ($\alpha^|$), austenite (γ) and cementite (θ). Carbon concentrations are in at.% and temperatures are in Kelvin.

	Specific Volume	Lattice parameter (Å)	Ref.	Linear thermal expansion coefficient (β, K^{-1})	Ref.
γ	$v_\gamma = {}^1\!/_4 \cdot a_\gamma^3$	$a_\gamma = 3.556 + 0.0453 \cdot x_c + 0.00095 \cdot x_{Mn}$	[29]	$1.244 \cdot 10^{-5}$	[30]
$\alpha^|$	$v_{\alpha^|} = {}^1\!/_2 \cdot c_{\alpha^|} \cdot a_{\alpha^|}{}^2$	$a_{\alpha^|} = 2.86640.0028 \cdot x_c$ $c_{\alpha^|} = 2.8664 + 0.0256 \cdot x_c$	[29]	$2.065 \cdot 10^{-5}$	[30]
θ	$v_\theta = {}^1\!/_{12} \cdot a_\theta \cdot b_\theta \cdot c_\theta$	$a_\theta = 5.0895, = 6.7449, = 4.5250$	[31]	$5.586 \cdot 10^{-6}$	[31]

Table 4
Experimental and calculated changes in length at the different partitioning temperatures (T_p) after 3600 s of partitioning time (t_p) in relation with the dominant phenomena occurring during the partitioning stage.

T_p, °C	Major phenomena	Experimental change in length (% ± 0.01%)	Theoretical change in length (%) at $t_p = 3600$ s
400	C-partitioning	0.029	0.032
450	C-partitioning; Carbide precipitation in γ	−0.023	−0.020
500	C-partitioning; Carbide precipitation in γ; Pearlite formation	−0.008	−0.017
550	C-partitioning; Carbide precipitation in γ; Pearlite formation	0.015	0.010
600	C-partitioning; Carbide precipitation in γ; Pearlite formation	−0.001	−0.002

Table 4 summarizes the major phenomena occurring at each partitioning temperature as well as the experimental and theoretical changes in length at the end of the partitioning step ($t_p = 3600$ s). The theoretical changes in length are calculated using equations 7 - 10 depending on the phases present at the respective partitioning temperature and using the data from Table 2. There exists a good agreement between the experimental and theoretical change in lengths, which indicates that the above-mentioned considerations, i.e. cementite as the carbide that precipitates inside primary martensite and from austenite, and complete carbon-depletion in primary martensite, are valid.

4.3. Analysis of simultaneous phenomena during high-temperature partitioning stages

It is well known that Q&P heat treatments aim to produce steels with good combinations of ductility and strength, which is achieved mainly from retained austenite and primary martensite, respectively [32–34]. In order to stabilize a significant fraction of retained austenite in the final microstructure it is important to avoid other reactions during the partitioning stage that might compete for the available carbon.

The microstructural evolution observed during partitioning at 400 °C confirms that the major phenomena occurring is the carbon partitioning from martensite to austenite, responsible for the retention of a volume fraction of austenite between 0.19 and 0.24 at room temperature after partitioning for 180 s and 3600 s, respectively. On the contrary, at 450 °C, an increase in partitioning time leads to a reduction in the volume fraction of retained austenite, while the fraction of fresh martensite, consequently, increases. This might be attributed to the precipitation of carbides in austenite during the partitioning stage, which reduces the total fraction of carbon available to stabilize the austenite at room temperature [35]. Considering the partitioning temperature of 500 °C, the maximum volume fraction of retained austenite is observed after partitioning for 180 s and the formation of pearlite is observed after 900 s. Whereas, at higher partitioning temperatures, 550 °C and 600 °C, pearlite is observed after 180 s of isothermal treatment and the volume fraction of retained austenite is lower than 0.05. The further increase in the isothermal holding time does not rise the volume fraction of re-

tained austenite; however, the pearlite volume fraction is observed to increase. It is evident that the microstructures show a tendency to form pearlite at high partitioning temperatures (500 °C - 600 °C). The formation of pearlite from the austenite grains during partitioning consumes part of the volume fraction of austenite and part of the carbon available for austenite stabilisation. Thus, the retained austenite fraction in the final Q&P microstructure is reduced.

As discussed earlier, the dilatometry analysis at the partitioning temperatures of 500 °C to 600 °C indicate that carbide precipitation inside austenite and pearlite formation occur simultaneously. The change in slopes of dilatometry curves during isothermal holding indicate a transition from a dominant process of carbide precipitation inside austenite (causing contraction) to a dominant process of pearlite formation (causing expansion). Fig. 5a,b and c show the dilatometry curve (red line), extrapolation of contraction (blue line) and expansion (green line) behaviour of the actual dilatometry curve at 500 °C, 550 °C and 600 °C respectively. By relating the final volume fraction of pearlite and the extrapolation of the dilatometry curve corresponding to pearlite formation (Fig. 5), the evolution of the volume fraction of pearlite with isothermal holding time at partitioning temperatures of 500 °C, 550 °C and 600 °C is calculated and shown in Fig. 6a. From Figs. 5 and 6a, the transition in the pre-dominant behaviour of carbide precipitation in austenite to pearlite formation during the partitioning stage is identified to be when the volume fraction of pearlite is in the range of 0.01 – 0.03.

For the investigated steel, the precipitation of carbides inside austenite seems to be unavoidable, as it occurs at the very early stage of the partitioning and as a result of the rapid carbon enrichment in austenite prompted at high partitioning temperatures. However, pearlite formation can be minimized to 0.01 volume fraction by restricting the isothermal holding to short times. Using information from Fig. 6a, the TTT diagram shown in Fig. 6b is constructed, where the partitioning times corresponding to pearlite volume fractions of 0.01 and 0.05 are indicated. It can be seen from Fig. 6b that, similar to what is predicted from the theoretical calculations using the MUCG83 program, the kinetics of pearlite formation is faster at partitioning temperatures around 550 °C (close to the nose of pearlite formation) than above or below.
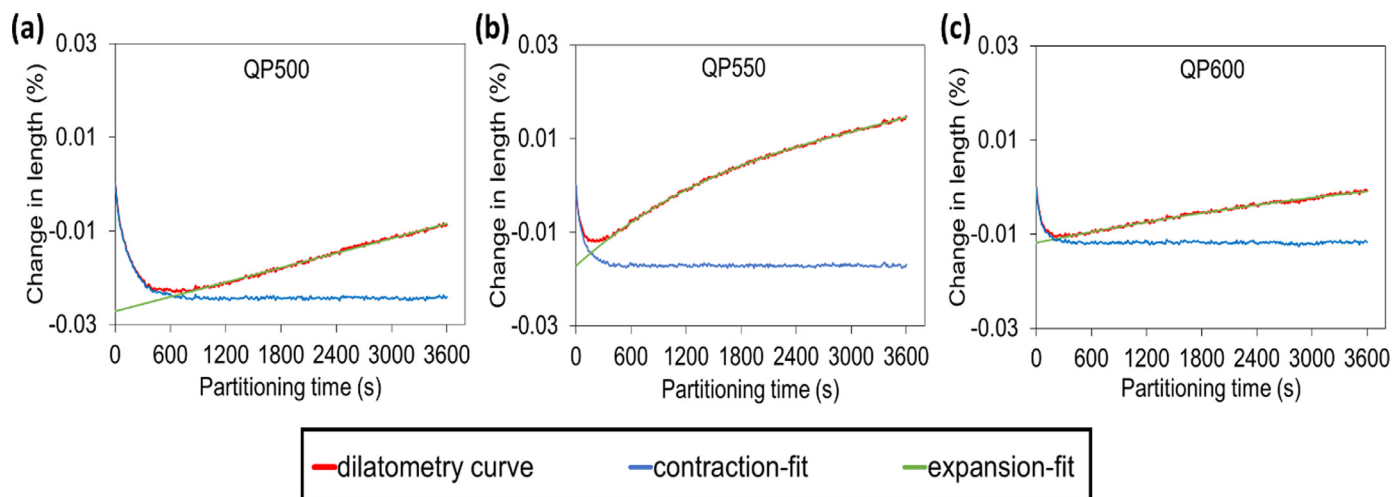
Fig. 5. Representation of change in length (red line) during isothermal holding at (a) 500 °C, (b) 550 °C and (c) 600 °C for 3600 s. The blue and green lines represent a polynomial fit for the observed contraction and expansion in the dilatometry curve, respectively. (For interpretation of the references to color in this figure legend, the reader is referred to the web version of this article.)
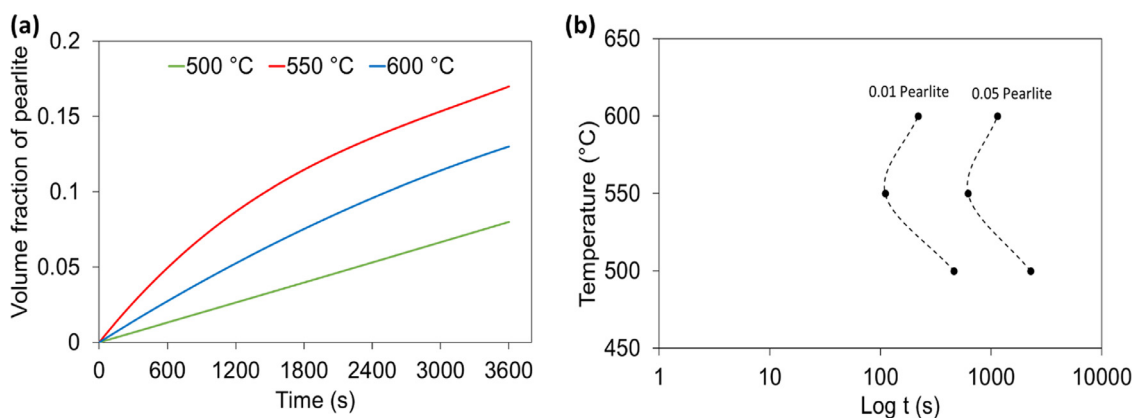

Fig. 6. (a) Volume fraction of pearlite formed during the isothermal holding at partitioning temperatures of 500 °C, 550 °C and 600 °C. (b) TTT diagram showing partitioning times corresponding to 0.01 and 0.05 volume fraction of pearlite formation during partitioning at 500 °C, 550 °C and 600 °C.

The morphology and location of the austenite after the initial quench seems to play a role in the degree of carbon enrichment during the partitioning step and, thus, in the precipitation of carbides or formation of pearlite within austenite. Based on the SEM observations, it is roughly estimated that around a 0.20 of the total volume fraction of the film-type of austenite is occupied with cementite. Assuming that the austenite surrounding the cementite particles is retained at room temperature and, hence, it has at least the minimum carbon content required for austenite stabilisation at room temperature (0.68 wt. % C as measured by XRD), carbon balance calculations yield that a carbon content of about 1.88 wt. % C is required so that a 0.20 volume fraction of cementite forms within a film of austenite. This carbon content is in good agreement with the results of carbon-redistribution simulations performed by Dictra at 500 °C by Hidalgo et al. [35].

In the case of pearlite, it is observed to nucleate along the prior austenite grain boundaries, where the diffusion of carbon is enhanced compared to that in bulk and, thus, a rapid carbon enrichment of the austenite can be expected at these locations. Yang et al. [18] reported that large austenite grains are highly favourable regions to form pearlite. Hidalgo et al. [35] showed by Dictra simulations that, at a partitioning temperature of 500 °C, austenite blocks of 0.3-0.5 μm in thickness can reach homogeneous carbon concentrations close to the eutectoid composition (0.80 wt% C) after 50 s of isothermal holding. This makes thermodynamically and kinetically possible the transformation of such

austenite into pearlite. At higher partitioning temperatures (550 °C and 600 °C), carbon diffuses even faster and tends to homogenize across the austenite grain in a shorter time, which would allow an earlier pearlite formation. Due to pearlite formation, the volume fraction of austenite available for stabilization through manganese partitioning is consumed.

In the case of partitioning at 500 °C–600 °C, manganese might have partitioned from martensite into austenite at the interfaces where no pearlite formation or carbide precipitation in austenite were observed. However, the austenite is not stabilized at room temperature (Table 2). This is because of insufficient carbon enrichment in the austenite during the partitioning stage due to pearlite formation or carbides precipitation in austenite. This indicates that, in the present case, though manganese is partitioned, it did not play a role in the austenite stabilization.

Based on the aforementioned analysis, the austenite stabilisation process might be enhanced during high-temperature partitioning provided the minimisation/suppression of competitive reactions. The formation of pearlite is pointed as the main process competing for the carbon available in the microstructure during the partitioning stage due to the large carbon contents and volume fractions of austenite that it consumes. To increase the fraction of retained austenite after the final quench, it is recommended to select relatively low quenching temperatures to create microstructures with a low volume fraction of untransformed austenite and small grain size which can 1) stabilize a high volume fraction of austenite during the final quench due to sufficient carbon enrichment

[36], 2) avoid pearlite formation when isothermal holding is restricted to short times. Carbide precipitation inside austenite is occurring in the initial stage of partitioning and seems to be unavoidable. However, an alloy with low carbon content (lower than that in the current work) might aid in delaying or suppressing carbide precipitation inside austenite by avoiding carbon supersaturation in austenite films.

5. Conclusions

The present study investigates the evolution of the microstructure during Quenching & Partitioning processing in a medium manganese steel at partitioning temperatures between 400 °C–600 °C and partitioning times up to 3600 s. The main conclusions extracted are:

- Partitioning at 400 °C leads to austenite stabilization through carbon partitioning, while partitioning at 450 °C leads to carbide precipitation inside austenite grains. At even higher partitioning temperatures (500 °C–600 °C) carbon partitioning also stimulates pearlite formation.
- Carbon balancing at partitioning temperatures of 400 °C–600 °C shows that almost no carbon is available in the primary martensite by the end of 3600 s of isothermal holding.
- High-partitioning temperatures (above 450 °C) result in a more rapid carbon partitioning kinetics than the usual 400 °C and provide sufficient driving force for the occurrence of additional reactions other than carbon partitioning. This results in carbide precipitation in austenite films and pearlite formation in austenite blocks depending on the morphology of the grain and partitioning conditions.
- Competitive phenomena, like carbide precipitation in austenite and pearlite formation, influence negatively the stabilisation of austenite, as they consume significant fractions of austenite and the carbon available for partitioning during the partitioning stage.
- For the current medium Mn steel, carbide precipitation in austenite and pearlite formation occur simultaneously during the partitioning stage. It is deduced that carbide precipitation in austenite and pearlite formation are dominant in the early and later stages of the partitioning stage, respectively.

The results of the current study provide better understanding of the microstructural changes that occur during Quenching and high-temperature partitioning processing (450 °C–600 °C) in medium Mn Q&P steels. It is understood that the suppression of the competitive reactions at high partitioning temperatures will help in optimizing the austenite stabilizing effect of carbon and manganese.

Declaration of Competing Interest

The authors declare that they have no known competing financial interests or personal relationships that could have appeared to influence the work reported in this paper.

Acknowledgments

Data availability

The raw and processed data required to reproduce these findings are available to download from doi:10.1016/j.mtla.2019.100492.

References

[1] J.G. Speer, A.M. Streicher, D. Matlock, F. Rizzo, G. Krauss, Quenching and partitioning: a fundamentally new process to create high strength trip sheet microstructures, Mater. Sci. Technol. Meet. (2003).

[2] D.V. Edmonds, K. He, M.K. Miller, F.C. Rizzo, A. Clarke, D.K. Matlock, J.G. Speer, Microstructural features of 'quenching and partitioning': a new martensitic steel heat treatment, Mater. Sci. Forum 539–543 (2007) 4819–4825.

[3] D.V. Edmonds, K. He, F.C. Rizzo, B.C. De Cooman, D.K. Matlock, J.G. Speer, Quenching and partitioning martensite—A novel steel heat treatment, Mater. Sci. Eng. A 438–440 (2006) 25–34.

[4] J.G. Speer, D.K. Matlock, B.C. De Cooman, J.G. Schroth, Carbon partitioning into austenite after martensite transformation, Acta Mater. 51 (9) (2003) 2611–2622.

[5] M. Gouné, F. Danoix, S.Y.P. Allain, O. Bouaziz, Unambiguous carbon partitioning from martensite to austenite in Fe–C–Ni alloys during quenching and partitioning, Scr. Mater. 68 (12) (2013) 1004–1007.

[6] F. HajyAkbary, J. Sietsma, G. Miyamoto, T. Furuhara, M.J. Santofimia, Interaction of carbon partitioning, carbide precipitation and bainite formation during the Q&P process in a low C steel, Acta Mater. 104 (2016) 72–83.

[7] D. Raabe, S. Sandlöbes, J. Millán, D. Ponge, H. Assadi, M. Herbig, P.P. Choi, Segregation engineering enables nanoscale martensite to austenite phase transformation at grain boundaries: a pathway to ductile martensite, Acta Mater. 61 (16) (2013) 6132–6152.

[8] M.J. Santofimia, L. Zhao, J. Sietsma, Microstructural evolution of a low-carbon steel during application of quenching and partitioning heat treatments after partial austenitization, Metall. Mater. Trans. A 40 (1) (2008) 46–57.

[9] M.J. Santofimia, L. Zhao, I. Povstugar, P.P. Choi, D. Raabe, J. Sietsma, Carbon redistribution in a quenched and partitioned steel analysed by atom probe tomography, in: N.H. Furuhara T, K Ushioda (Eds.), Proceedings of the 3rd International Symposium Steel Science (ISSS), The Iron and Steel Institute of Japan, Kyoto, 2012, p. 155.

[10] D. De Knijf, M.J. Santofimia, H. Shi, V. Bliznuk, C. Föjer, R. Petrov, W. Xu, In situ austenite–martensite interface mobility study during annealing, Acta Mater. 90 (2015) 161–168.

[11] M. Gouné, S. Aoued, F. Danoix, G. Geandier, A.Q. Poulon, J.C. Hell, M. Soler, S.Y.P. Allain, Alloying-element interactions with austenite/martensite interface during quenching and partitioning of a model Fe–C–Mn–Si alloy, Scr. Mater. 162 (2019) 181–184.

[12] E.J. Seo, L. Cho, B.C. De Cooman, Kinetics of the partitioning carbon and substitutional alloying elements during quenching and partitioning (Q&P) processing of medium mn steel, Acta Mater. 107 (2016) 354–365.

[13] Y. Toji, H. Matsuda, M. Herbig, P.P. Choi, D. Raabe, Atomic-scale analysis of carbon partitioning between martensite and austenite by atom probe tomography and correlative transmission electron microscopy, Acta Mater. 65 (2014) 215–228.

[14] T.Inoe Tschiyama, J. Tobata, D. Akami, S. Takaki, Microstructure and mechanical properties of a medium manganese steel treated with interrupted quenching and intercritical annealing, Scr. Mater. 122 (2016) 36–39.

[15] R. Ding, Z. Dai, M. Huang, Z. Yang, C. Zhang, H. Chen, Effect of pre-existed austenite on austenite reversion and mechanical behaviour of an Fe-0.2C-8Mn-2Al medium mn steel, Acta Mater. 147 (2018) 59–69.

[16] J. Ågren, A revised expression for the diffusivity of carbon in binary Fe-C austenite, Scr. Metall. 20 (11) (1986) 1507–1510.

[17] H. Oikawa, Review on lattice diffusion of substitutional impurities in iron. A summary report, Technol. Rep. Tohoku Univ. 47 (2) (1982) 215–224.

[18] J.R. Yang, H.K.D.H. Bhadeshia, Continuous heating transformation of bainite to austenite, Mater. Sci. Eng. A131 (1991) 99–113.

[19] C.F. Jatczak, Retained Austenite and Its Measurement By X-Ray Diffraction, SAE International, 1980.

[20] N. Vandijk, A. Butt, L. Zhao, J. Sietsma, S. Offerman, J. Wright, S. Vanderzwaag, Thermal stability of retained austenite in trip steels studied by synchrotron X-ray diffraction during cooling, Acta Mater. 53 (20) (2005) 5439–5447.

[21] L. Zhao, N.H. Van Dijk, E. Bruck, J. Sietsma, S. Van der Zwaag, Magnetic and X-ray diffraction measurements for the determination of retained austenite in trip steels, Mater. Sci. Eng. A 313 (1) (2001) 145–152.

[22] S.M.C. Van Bohemen, D.N. Hanlon, A physically based approach to model the incomplete bainitic transformation in high-Si steels, Int. J. Mater. Res. 103 (8) (2012) 987–991.

[23] S.M.C. Van Bohemen, Austenite in multiphase structures quantified by analysis of thermal expansion, Scr. Mater. 75 (2014) 22–25.

[24] M.J. Santofimia, L. Zhao, J. Sietsma, Volume change associated to carbon partitioning from martensite to austenite, Mater. Sci. Forum 706-709 (2012) 2290–2295.

[25] R. Kannan, Y. Wang, L. Li, Identification of inverse bainite in fe-0.84c-1cr-1mn hypereutectoid low alloy steel, Metall. Mater. Trans. A 48A (2017) 948–952.

[26] M. Onink, C.M. Brakrnan, F.D. Tichelaar, E.J. Mittemeijer, S. Van der Zwaag, The lattice parameters of austenite and ferrite in Fe-C alloys as functions of carbon concentration and temperature, Scr. Metall. Mater. 29 (1993) 1011–1016.

[27] E.S. Rowland, S.R. Lyle, The application of MS points to case depth measurement, Trans. ASM 37 (1946) 27–47.

[28] H.K.D.H. Bhadeshia, A thermodynamic analysis of isothermal transformation diagrams, Met. Sci. 16 (1982) 159–165.

[29] L. Cheng, A. Böttger, T.H. de Keijser, E.J. Mittemeijer, The tempering of iron carbon martensite dilatometric and calorimetric analysis, Metall. Trans. A 19 (10) (1988) 2415–2426.

[30] C. Garcia de Andres, F.G. Caballero, C. Capdevila, L.F. Alvarez, Application of dilatometric analysis to the study of solid–solid phase transformations in steels, Mater. Charact. 48 (1) (2002) 101–111.

[31] S. Hartmann, H. Ruppersberg, Thermal expansion of cementite and thermoelastic stresses in white cast iron, Mater. Sci. Eng. A 190 (1) (1995) 231–239.

[32] Sung-Joon Kim, Chang Gil Lee, Tae-Ho Lee, Chang-Seok Oh, Effect of Cu, Cr and Ni on mechanical properties of 0.15 wt% C TRIP-aided cold rolled steels, Scr. Mater. 48 (2003) 539–544.

[33] H. Jirková, L. Kučerová, B. Mašek, Effect of quenching and partitioning temperatures in the Q-P process on the properties of ahss with various amounts of manganese and silicon, Mater. Sci. Forum 706–709 (2012) 2734–2739.

[34] N. Zhu, Q. Wu, Y. He, X. Lu, L. Li, P. Hu, Effect of ni on the stability of retained austenite and mechanical properties for trip steels containing vanadium, Steel Res. Int. 85 (2) (2014) 143–154.

[35] J. Hidalgo, C. Celada-Casero, M.J. Santofimia, Fracture mechanisms and microstructure in a medium MN quenching and partitioning steel exhibiting macrosegregation, Mater. Sci. Eng. A 754 (2019) 766–777.

[36] C. Celada-Casero, J. Sietsma, M.J. Santofimia, The role of the austenite grain size in the martensitic transformation in low carbon steels, Mater. Des. 167 (2019) 107625.